VOLUME ABSORPTION AND VOLUME REVERBERATION DUE TO MICROBUBBLES AND SUSPENDED PARTICLES IN A RAY-BASED SONAR PERFORMANCE MODEL

S.D. Richards[1], P.R. White[2] and T.G. Leighton[2]

[1]Marine and Acoustics Centre, QinetiQ, Winfrith Technology Centre, Dorchester, Dorset DT2 8XJ, United Kingdom.
[2]Institute of Sound and Vibration Research, University of Southampton, Highfield, Southampton, SO17 1BJ, United Kingdom.
E-mail: sdrichards@QinetiQ.com, prw@isvr.soton.ac.uk, tgl@soton.ac.uk

Suspended solid particles and microbubbles cause absorption and scattering of underwater sound. Such inhomogeneities can therefore contribute to both the volume attenuation and the volume reverberation level, as well as modifying the speed of sound. These effects have been added to a ray-based sonar model, and results are presented which demonstrate their significance for high frequency sonar performance prediction.

1. INTRODUCTION

Shallow coastal waters may be characterized by relatively high concentrations (although they may still be considered acoustically as dilute populations) of suspended mineral particles, and microbubbles extending throughout the water column. Current sonar performance models do not explicity include the effects of these inhomogeneities on the volume attenuation coefficient, the sound speed profile, or the volume reverberation level.

2. SOLID PARTICLES

Solid particles suspended in a fluid can influence acoustic propagation in a number of ways, including increasing the attenuation through visco-inertial absorption, thermal absorption, and scattering, increasing the volume reverberation and modifying the sound speed. For mineral particles suspended in seawater at practical sonar frequencies, thermal absorption, reverberation and sound speed variations due to dilute suspensions can generally be neglected [1].

The attenuation coefficient due to the particles may therefore be expressed as $\alpha = \alpha_v + \alpha_s$, where α_v and α_s are the contributions due to visco-inertial absorption and scattering, respectively.

2.1. Visco-inertial absorption

Urick [2] found the following expression for the visco-inertial attenuation coefficient

$$\frac{\alpha_v}{10 \log \mathrm{e}^2} = \frac{\phi k(\sigma - 1)^2}{2} \left[\frac{s}{s^2 + (\sigma + \tau)^2} \right], \tag{1}$$

where

$$\tau = \frac{1}{2} + \frac{9}{4} \left(\frac{\delta_\mathrm{v}}{a} \right) \quad \text{and} \quad s = \frac{9}{4} \left(\frac{\delta_\mathrm{v}}{a} \right) \left(1 + \frac{\delta_\mathrm{v}}{a} \right). \tag{2}$$

Here ϕ is the volume fraction of suspended particles, k is the acoustic wavenumber, σ is the ratio of the densities of the solid and fluid phases, a is the particle radius and $\delta_\mathrm{v} = \sqrt{2\nu/\omega}$ is the skin depth for shear waves, where ν is the kinematic viscosity of the fluid and ω is the acoustic frequency. This absorption coefficient, in common with other attenuation coefficients in this paper, is expressed in dB.

2.2. Scattering

Sheng and Hay [3] have constructed a high pass model for the attenuation coefficient due to scattering, which can be written as

$$\frac{\alpha_\mathrm{s}}{10 \log \mathrm{e}^2} = \frac{\epsilon K_\alpha x^4}{a \left(\frac{4}{3} K_\alpha x^4 + \xi x^2 + 1 \right)}, \tag{3}$$

where $x = ka$,

$$K_\alpha = \frac{1}{6} \left(\gamma_\kappa^2 + \frac{\gamma_\rho^2}{3} \right), \tag{4}$$

and ξ is an adjustable constant ≥ 1. The ξ term allows the form of the polynomial to be adjusted to improve the fit to experimental data for intermediate x values. The terms γ_κ and γ_ρ are, respectively, compressibility and density contrasts [3].

3. MICROBUBBLES

As with solid particles, the presence of microbubbles in the water column leads to additional acoustic attenuation through thermal and viscous absorption and scattering. Unlike particles, however, resonant scattering can be important in the case of bubbles, and the scattering cross-section of a bubble near resonance may be very much larger than its geometric cross-section. Bubbles also cause the compressibility of the medium to be complex, in the linear representation, resulting in dispersion.

Whilst the additional reverberation due to solid particles is small and can generally be neglected, the bubbles' contribution to volume reverberation may be significant and should be taken into account.

3.1. Dispersion relation

The dispersion relation for a bubbly liquid may be written [4]

$$k_{\mathrm{b}}^2 = \frac{\omega^2}{c^2} + 4\pi\omega^2 \int_{a_0=0}^{\infty} \frac{a_0 n_{\mathrm{b}}(a_0) da_0}{\omega_0^2 - \omega^2 + 2\mathrm{i}b\omega}, \tag{5}$$

where k_{b} is the complex wavenumber for the bubbly liquid, ω is the angular frequency of the acoustic wave, c is the speed of sound in the ambient fluid, a_0 is the equilibrium bubble radius, ω_0 is the resonant frequency of bubbles having equilibrium radius a_0 and $n_{\mathrm{b}}(a_0) da_0$ is the number of bubbles per unit volume in the size range a_0 to $a_0 + da_0$ (it is conventional to take $da_0 = 1~\mu\mathrm{m}$). The damping constant b is a summation of the viscous, thermal and radiation damping of the bubble, given by [4].

The phase speed c_{b} and attenuation coefficient α_{b} for the bubbly liquid may be obtained from the real and imaginary parts of the complex wavenumber (Equation 5) using the following relation

$$k_{\mathrm{b}} = \frac{\omega}{c_{\mathrm{b}}} + \frac{\mathrm{i}\alpha_{\mathrm{b}}}{10 \log \mathrm{e}^2}. \tag{6}$$

3.2. Reverberation

The linear, steady-state, monochromatic scattering cross-section of an individual bubble, Ω_{bub}, at frequency f is given by

$$\Omega_{\mathrm{bub}}(f, a_0) = 4\pi a_0^2 \left[\left(\frac{f_0^2}{f^2} - 1 \right)^2 + b^2 \right]^{-1}, \tag{7}$$

where f_0 is the bubble's resonant frequency, a_0 is its equilibrium radius and b is the total damping constant at resonance. This assumes omni-directional scattering and is thus valid for $ka_0 \ll 1$ [5, 6]. For an illustration of the non-linear cross-section, see Leighton *et al.* in these proceedings.

The linear, monochromatic scattering cross-section of a bubble field, per unit volume, is given by

$$\Omega_{\mathrm{vol}}(f) = \frac{1}{4\pi} \int_0^{\infty} \Omega_{\mathrm{bub}}(f, a_0) n_{\mathrm{b}}(a_0) da_0. \tag{8}$$

In shallow water, the resonant frequency can be related to the equilibrium radius through the approximate relationship [5, 6] $f_0 = 3.25/a_0$, and combining this with Equations 7 and 8 leads to the expression

$$\Omega_{\mathrm{vol}}(f) = \int_0^{\infty} a_0^2 \left[\left(\frac{3.25^2}{a_0^2 f^2} - 1 \right)^2 + b^2 \right]^{-1} n_{\mathrm{b}}(a_0) da_0. \tag{9}$$

The damping coefficient can also be approximated in terms of the bubble radius through [6]

$$b = 0.0025 f_0^{1/3} = 0.0025(3.25/a_0)^{1/3} = 0.0037/r^{1/3} \tag{10}$$

The bubble population implemented here is an empirical approximation to the data of Farmer *et al.* [7]:

$$n_{\mathrm{b}}(a_0, z, w) = Bw^{1/2} \exp\left(-z/D_{\mathrm{e}}\right) p(R_0),$$ (11)

with

$$p(R_0) = \left\{ \begin{array}{ll} R_0^{-p_1} & R_0 \leq R_{\mathrm{ref}} \\ \beta R_0^{-p_2} & R_0 > R_{\mathrm{ref}} \end{array} \right. ,$$ (12)

where w is the wind speed at 10 m, z is the depth below the instantaneous sea surface, D_{e} is the e-folding depth, and R_0 is the equilibrium bubble radius in μm. Farmer found that $R_{\mathrm{ref}} = 100$ μm was appropriate for the measured data, with $p_1 = -1.75$ and $p_2 = 5.0$. The parameter $\beta = R_{\mathrm{ref}}^{(p_2-p_1)} = R_{\mathrm{ref}}^{6.75}$ is adjusted to ensure continuity at R_{ref}, and $B = 4094$. It should be emphasized that this is a simplification. For example there is some evidence that R_{ref} decreases somewhat with depth, and this has not been included. There is also systematic evolution of the bubble size spectrum with time following injection by a breaking wave. The e-folding depth found by Farmer was $D_{\mathrm{e}} = 0.7$ m.

4. RESULTS

The acoustic environment is modelled here using ray tracing to determine sound paths in a horizontally stratified water column. The signal-to-noise ratio (SNR) along each ray is determined by calculating the directivity, absorption, geometric spreading loss, the effects of various noise and reverberation sources, and applying the active sonar equation.

In order to include the additional effects of suspended particles and microbubbles into the model, the density and viscosity of the water must be known. The density and viscosity profiles are therefore calculated in the model from the temperature profile and salinity. This approach ensures that all of the water column properties are consistent with each other. The expressions used to calculate density and viscosity as functions of temperature, pressure and salinity are given in [9].

The basic situation which is modelled here is a typical monostatic, shallow water, high frequency sonar scenario [1]. The sonar is at a depth of 10 m in water of depth 40 m, and the centre frequency is 100 kHz. The water column is isovelocity in the absence of the bubbles.

Fig. 1 shows that these suspended particle and bubble populations have a significant effect on the SNR in this modelled scenario. If it is assumed that the detection range for this particular sonar system is defined as the range beyond which the SNR drops below 0 dB then it may be seen from the figure that the detection range would be in excess of 500 m in clear water. This drops to less than 400 m in the presence of the chosen population of suspended particles and is reduced to less than 300 m in the presence of the modelled bubble population. If both suspended particles and bubbles are included in the model then the detection range is less than 250 m. Note that for a real sonar system the lowest SNR at which detection is possible depends on a number of factors, including the signal processing, and the required probability-of-detection and probability-of-false alarm.

Fig. 2 demonstrates the effects of bubbles on the volume reverberation in a typical high frequency sonar scenario. Note that this is a different scenario than was used to produce Fig. 1. In this case the water depth is 100 m, there is a symmetric bilinear sound speed profile with a minimum at 50 m, and the centre frequency is 80 kHz. Fig. 2a shows the ray paths, computed here without bubbles (but the addition of the bubble population used here does not alter the
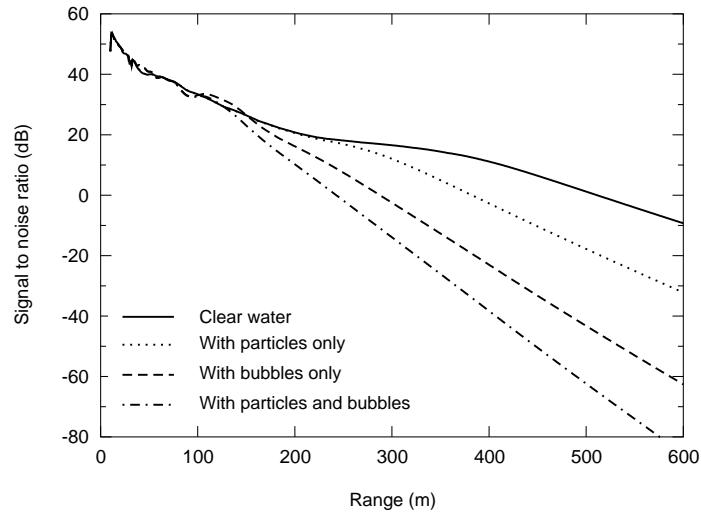
Fig. 1: Signal-to-noise ratio for a typical high frequency sonar scenario (see text) showing the effects of suspended particles and microbubbles.
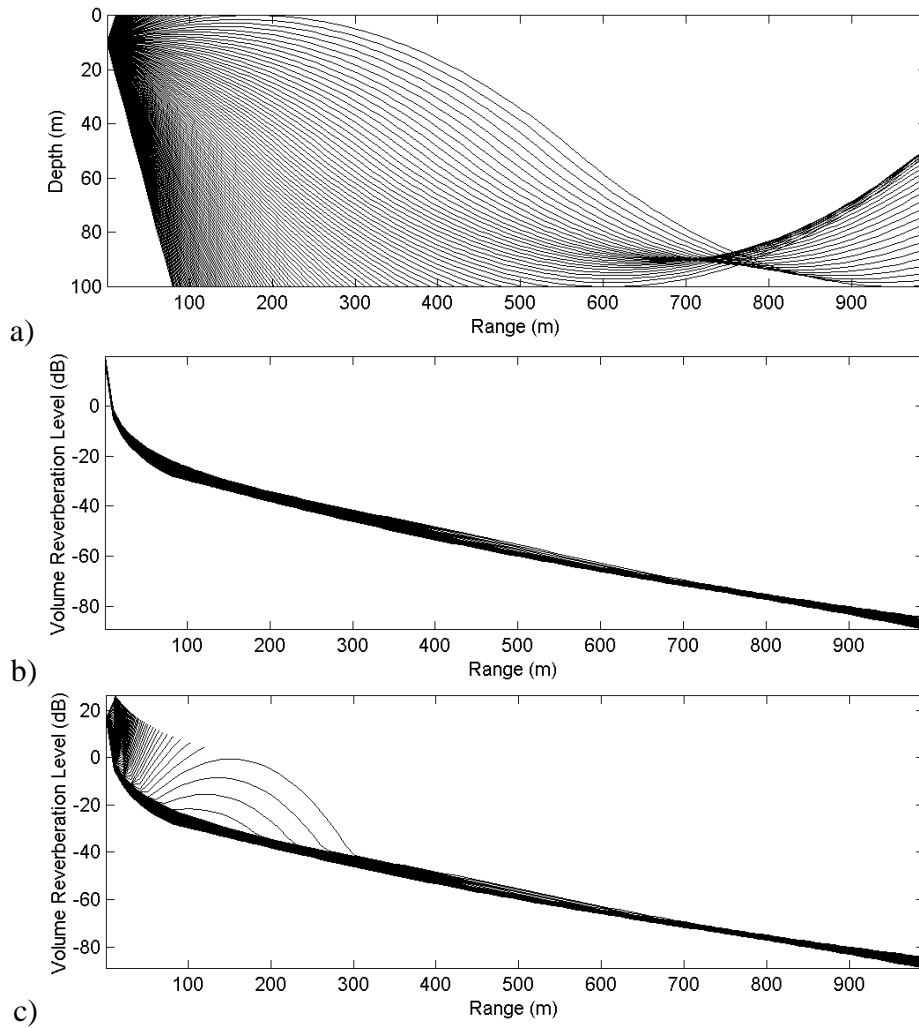

Fig. 2: a) Modelled ray paths; and volume reverberation level as a function of range for each ray in the simulation: b) no bubbles; c) including bubbles.

ray paths appreciably). Fig. 2b shows the case without including bubbles, in which the volume scattering strength is assumed to be constant (i.e. a homogenous distribution of scatterers). The reverberation level is plotted as a function of range for each ray traced in the model, and the small variation in level between rays results from differences in the path length between rays for a given horizontal range. Fig. 2b shows the result of including the bubbles, illustrating the increase in volume reverberation in rays which pass close to the sea surface, where the bubble density is significant. This implies that early reverberation returns will be significantly enhanced by scattering from bubbles in the surface layers, as is to be expected.

5. CONCLUSIONS

The additional attenuation due to suspended mineral particles and microbubbles has been incorporated into a ray-method sonar performance prediction model, along with the effect of microbubbles on the sound speed profile and volume reverberation level.

Results demonstrate that both suspended mineral particles and microbubbles can have a significant impact on high frequency sonar performance, and should therefore be included in sonar performance predictions for shallow, turbid environments.

6. ACKNOWLEDGEMENTS

REFERENCES

[1] **Richards S.D.**, Visco-inertial absorption in dilute particulate suspensions, *Ph.D. Thesis*, University of Southampton, 2002.

[2] **Urick R. J.**, The absorption of sound in suspensions of irregular particles, *J. Acoust. Soc. Am.*, 20, pp. 283–289, 1948.

[3] **Sheng J. and Hay A.E.**, An examination of the spherical scatterer approximation in aqueous suspensions of sand, *J. Acoust. Soc. Am.*, 85, pp.598–610, 1988.

[4] **Commander K.W. and Prosperetti A.**, Linear pressure waves in bubbly liquids: Comparison between theory and experiments, *J. Acoust. Soc. Am.*, 85, pp. 732–746, 1989.

[5] **Leighton T.G.**, *The Acoustic Bubble*, Academic Press, 1994.

[6] **Medwin H. and Clay C.S.**, *Fundamentals of Acoustical Oceanography*, Academic Press, 1998.

[7] **Farmer D.M., Vagle S. and Booth A.D.**, A free-flooding acoustical resonator for measurement of bubble size distribution, *J. Atmospheric & Oceanic Technology*, 15, pp. 1132–1145, 1998.

[8] **Del Grosso V.A.**, New equation for the speed of sound in natural waters (with comparisons to other equations), *J. Acoust. Soc. Am.*, 56, pp. 1084–1091, 1974.

[9] **Richards S.D.**, The effect of temperature, pressure and salinity on sound attenuation in turbid seawater, *J. Acoust. Soc. Am.*, 103, pp. 205–211, 1998.